

## Anomaly in the differential cross sections at 13 TeV

O. V. Selyugin\*

*BLTP, Joint Institute for Nuclear Research, 141980 Dubna, Moscow region, Russia*

The analysis of the new TOTEM data at 13 TeV in a wide momentum transfer region reveals the unusual phenomenon - the presence in the elastic scattering amplitude of a term with a very large slope that is responsible for the behavior of hadron scattering at a very small momentum transfer. This term can be connected with hadron interactions at large distances.

13.40.Gp, 14.20.Dh, 12.38.Lg

### 1. Introduction

The new data of the TOTEM Collaboration on the elastic differential cross sections at 13 TeV have two sets of data - at small momentum transfer <sup>1</sup> and at middle and large momentum transfer <sup>2</sup>. Recently, the first set of data has created a wide discussion of the determination of the total cross section and the value of  $\rho(t=0)$  (for example <sup>3,4,5</sup>). A research of the structure of the elastic hadron scattering amplitude at superhigh energies and small momentum transfer -  $t$  can give a connection between the experimental knowledge and the basic asymptotic theorems based on first principles <sup>6,7,8</sup>. It gives information about the hadron interaction at large distances where the perturbative QCD does not work <sup>9</sup>, and a new theory as, for example, instanton or string theories must be developed.

Usually, a small region of  $t$  is taken into account for extraction of the sizes of  $\sigma_{tot}$  and  $\rho(t=0)$  (for example <sup>1,10</sup>). Really, already in the analysis of the UA4/2 data it was shown that the value of  $\rho(s,t)$  has a phenomenological meaning, as its determination requires some model assumptions <sup>11</sup>. A simple exponential approximation of the data gave  $\rho = 0.24$  from the UA4 data and  $\rho = 0.129$  from UA4/2 data (both at  $\sqrt{s} = 540$  GeV. More complicated analyses gave  $\rho = 0.19$  from the UA4 data and  $\rho = 0.16$  from UA4/2 data <sup>11</sup>. Hence, this is not an experimental problem but a theoretical one <sup>12</sup>. A phenomenological form of the scattering amplitude determined for small  $t$  can lead to very different differential cross sections at larger  $t$ . Especially, it is connected with the differential cross section at 13 TeV, as the diffraction minimum is located at a non-large  $t$ .

Also, a very important moment is related with the question how the experimental uncertainty, which is usually named experimental errors, is used in our fitting

\**selyugin@theor.jinr.ru*

procedure. In fact, the actual background rates and shapes of the measured distributions are sensitive to a number of experimental quantities such as calibration constants, detector geometries, poorly known material budgets within experiments, particle identification efficiencies, etc. A 'systematic error', referred to by a high energy physicist, usually corresponds to a 'nuisance parameter' by a statistician.

Hence, the extraction of the main value of the elastic hadron interaction requires some model that can describe all experimental data at the quantitative level with minimum free parameters. Now many groups of researchers have presented some physical models satisfying more or less these requirements. It is especially related with the HEGS (High Energy Generalized Structure) model<sup>13,14</sup>. As it takes into account two form factors (electromagnetic and gravitomagnetic), which are calculated from the GPDs function of nucleons, it has a minimum free parameters and gives a quantitative description of the existing experimental data in a wide energy region and momentum transfer. Analysis of new data of the TOTEM Collaboration at 13 TeV in the framework of the HEGS model discovered a new phenomenon in the hadron interaction - the oscillation term of the elastic scattering amplitude<sup>15</sup>. During this analysis only statistical errors of experimental data were taken into account in the fitting procedure. Systematic errors were taken as an additional coefficient of the normalization of the differential cross section, which is independent of the momentum transfer.

Further careful analysis of the behavior of the differential cross sections in the framework of the HEGS model have shown additional unusual properties of the behavior of the elastic scattering amplitude at a very small momentum transfer. The effect is examined from different points of view in the present paper.

In the second section of the paper, the new effect is analyzed in the framework of the HEGS model with taking into account experimental data of both the sets of the TOTEM Collaboration obtained at 13 TeV and is compared with the results of some other models in the third section. In the fourth section, the existence of the new effect is examined in a simple phenomenological form of the scattering amplitude (as used most groups of researchers) and experimental data of only the first set at small momentum transfer are taken into account. The conclusions are given in the final section.

## **2. Some problems in the description of the differential cross section in a wide region of momentum transfer**

There are many different semi-phenomenological models which give a qualitative description of the behavior of the differential cross sections of the elastic proton-proton scattering at  $\sqrt{s} = 13$  TeV (for example<sup>16,17,18</sup>). Some examples can be found in the review<sup>19</sup>; hence, we do not give a deep analysis of those models. One of the common properties of practically all models is that they take into account statistical and systematic errors in quadrature form and, in most part, give only a qualitative description of the behavior of the differential cross section in a wide

momentum transfer region.

However, there are two essentially different ways of including statistical and systematic uncertainties in the fitting procedure, especially if we want to obtain a quantitative description of experimental data. The first one, mostly used in connection with the differential cross sections (for example <sup>20,21,17,16</sup>), takes into account statistical and systematic errors in quadrature form:  $\sigma_{i(tot)}^2 = \sigma_{i(stat)}^2 + \sigma_{i(syst)}^2$ . In this case,  $\chi^2$  can be simply written as

$$\chi^2 = \sum_{i=1}^n \frac{(\hat{E}_i - F_i(\vec{a}))^2}{\sigma_{i(tot)}^2}. \quad (1)$$

The second approach accounts for the basic property of systematic uncertainties, i.e. the fact that these errors have the same sign and size in proportion to the effect in one set of experimental data and possibly have a different sign and size in another set. To account for these properties, extra normalization coefficients  $k_j = 1 + \sigma$  for the measured data are introduced in the fit. For simplicity, this normalization is often transferred into the model parametrization  $f_j = 1/k_j$ , while it - in reality - accounts for the uncertainty of the normalization of experimental data. <sup>22</sup>. This method is often used by research collaborations to extract, for example, the parton distribution functions of nucleons <sup>23,24</sup> and nuclei <sup>25</sup> in high energy accelerator experiments, or in astroparticle physics <sup>26</sup>. In this case,  $\sigma_{i(tot)}^2 = \sigma_{i(stat)}^2$  and the systematic uncertainty are taken into account as an additional normalization coefficient, with inverse form  $f = 1/k$ . <sup>22</sup>. Hence, systematic errors can be represented as an additional normalization coefficient. Then, only statistical errors have to be taken into account in calculations of  $\chi^2$ .

$$\chi^2 = \sum_{j=1}^m \left[ \sum_{i=1}^n \frac{(\hat{E}_{ij} - f_j F_{ij})^2}{\sigma_{ij(st.)}^2} + \frac{(1 - f_j)^2}{\sigma_j^2} \right]. \quad (2)$$

It should be noted that in the minimization procedure used in these two methods, different sizes of experimental errors were assumed. In the first case, we account for experimental errors in the quadrature of statistical and systematic errors and for experimental data with the normalization given by an experimental collaboration. In the second case, only statistical errors are considered as experimental uncertainty. The systematic errors are accounted for as an additional normalization coefficient interpreted as a nuisance parameter applied to all experimental data of this separate data set.

In the first case, the "quadrature form" of the experimental uncertainty gives a wide corridor in which different forms of the theoretical amplitude can exist. In the second case, the "corridor of the possibility" is essentially narrow, and it restricts different forms of theoretic amplitudes.

To examine subtle effects in the behavior of differential cross sections, it is needed to have the narrowest possible corridor for testing a theoretical function. In our paper <sup>15</sup>, it was shown that the new data of the TOTEM Collaboration at 13 TeV show the existence in the scattering amplitude of the oscillation term, which can

be determined by the hadron potential at large distances. In the analysis of experimental data of both the sets of the TOTEM data the additional normalization was used. Its size reaches sufficiently large values. In this case, a very small  $\chi_{dof}^2$  was obtained with taking into account only statistical errors and with a small number of free parameters in the scattering amplitude, which was obtained in our High Energy Generalized Structure (HEGS) model<sup>13,14</sup>. However, the additional normalization coefficient reaches a sufficiently large value, about 13%. It can be in a large momentum transfer region but is very unusual for a small momentum transfer. However, both sets of experimental data (small and large region of  $t$ ) overlap in some region and, hence, affect each other's normalization. It is to be noted, that the size of the normalization coefficient does not impact the size and properties of the oscillation term. We have examined many different variants of our model (including large and unity normalization coefficient), but the parameters of the oscillation term have small variations.

In the present work, the analysis of both sets of the TOTEM data at 13 TeV is carried out with additional normalization equal to unity and taking into account only statistical errors in experimental data. Hence, the additional normalization coefficient in eq.(2) are fixed by unity  $f_j = 1$ . In the work, the fitting procedure uses the modern version of the program "FUMILIM"<sup>27,28</sup> of the old program "FUMILY"<sup>29</sup> which calculates the covariant matrix and gives the corresponding errors of parameters and their correlations coefficients, and the errors of the final data. The analysis of the TOTEM data by three different statistical methods, including the calculations through the correlation matrix of the systematic errors was made in<sup>30</sup>

### 3. Model description of two sets at 13 TeV with additional normalization equal to unity

Differential cross sections measured experimentally are described by the squared scattering amplitude

$$\begin{aligned} d\sigma/dt = \pi (F_C^2(t) + (1 + \rho^2(s, t)) \text{Im}F_N^2(s, t) \\ \mp 2(\rho(s, t) + \alpha\varphi) F_C(t)\text{Im}F_N(s, t)). \end{aligned} \quad (3)$$

where  $F_C = \mp 2\alpha G^2/|t|$  is the Coulomb amplitude;  $\alpha$  is the fine-structure constant,  $\varphi(s, t)$  is the Coulomb hadron interference phase between the electromagnetic and strong interactions (in our case, it is taken from<sup>31,32,33</sup>), and  $\text{Re} F_N(s, t)$  and  $\text{Im} F_N(s, t)$  are the real and imaginary parts of the nuclear amplitude;  $\rho(s, t) = \text{Re} F(s, t)/\text{Im} F(s, t)$ . Just this formula is used to fit experimental data determined by the Coulomb and hadron amplitudes and the Coulomb-hadron phase to obtain the value of  $\rho(s, t)$ .

As a basis, we take our high energy generalized structure (HEGS) model<sup>13,14</sup> which quantitatively describes, with only a few parameters, the differential cross section of  $pp$  and  $p\bar{p}$  from  $\sqrt{s} = 9$  GeV up to 13 TeV, includes the Coulomb-hadron

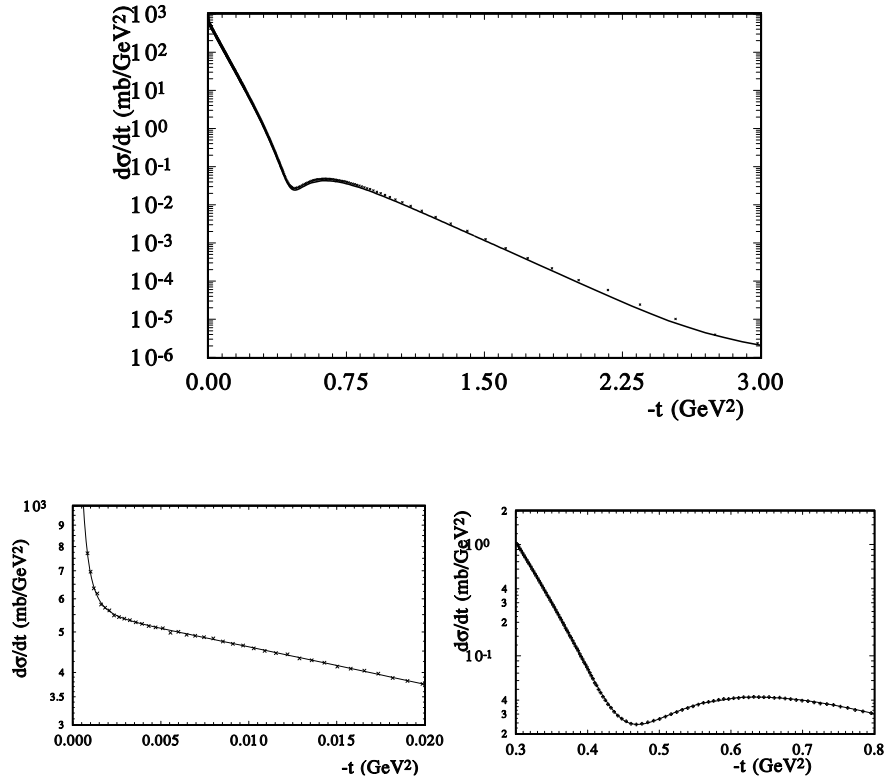


Fig. 1. The differential cross sections are calculated in the framework of the HEGS model with fixed additional normalization by 1.0 and with additional term eq.(7), a) [top] the full region of  $t$  and the data [1,2] b) [bottom-left] the magnification of the region of the small momentum transfer of a); c) [bottom-right] the magnification of the region of the diffraction minimum.

interference region and the high- $|t|$  region up to  $|t| = 15$  GeV<sup>2</sup> and quantitatively well describes the energy dependence of the form of the diffraction minimum<sup>34</sup>. However, to avoid possible problems connected with the low-energy region, we consider here only the asymptotic variant of the model.

The total elastic amplitude in general receives five helicity contributions, but at high energy it is enough to write it as  $F(s, t) = F^h(s, t) + F^{\text{em}}(s, t)e^{\varphi(s, t)}$ , where  $F^h(s, t)$  comes from the strong interactions and  $F^{\text{em}}(s, t)$  from the electromagnetic interactions. Note that all five spiral electromagnetic amplitudes are taken into account in the calculation of the differential cross sections. The Born term of the elastic hadron amplitude at large energy can be written as a sum of two pomeron

and odderon contributions,

$$F_{\mathbb{P}}(s, t) = \hat{s}^{\epsilon_0} \left( C_{\mathbb{P}} F_1^2(t) s^{\alpha' t} + C'_{\mathbb{P}} A^2(t) \hat{s}^{\frac{\alpha' t}{4}} \right), \quad (4)$$

$$F_{\mathbb{O}}(s, t) = i \hat{s}^{\epsilon_0 + \frac{\alpha' t}{4}} (C_{\mathbb{O}} + C'_{\mathbb{O}} t) A^2(t). \quad (5)$$

All terms are supposed to have the same intercept  $\alpha_0 = 1 + \epsilon_0 = 1.11$ , and the pomeron slope is fixed at  $\alpha' = 0.24 \text{ GeV}^{-2}$ . Many models used the electromagnetic form factors of the hadron for the description of the scattering amplitude but, in most part, they changed their form to describe experimental data, as was made in the famous Bourrely-Soffer-Wu model <sup>37</sup>. The parameters of the obtained form-factor are determined by fitting of the differential cross sections. The authors noted that the form factor is "parameterized like an electromagnetic form factor, as two poles, and the slowly varying function reflects the approximate proportionality between the charge density and hadronic matter distribution inside a proton."

In paper <sup>38</sup>, it was proposed that the hadron form factor is proportional to the matter distribution. The matter distributions in the hadron are tightly connected with the energy momentum tensor <sup>39</sup>. In <sup>40</sup>, it was noted that "the gravitational form factors are related to the matrix elements of the energy-momentum tensor in a hadronic state, thus providing the distribution of matter within the hadron". The recent picture of the hadron structure is determined by the general parton distributions (GPDs) <sup>41,42</sup> which include, as part, the parton distribution functions (PDFs).

In the HEGS model the form factors are determined by the general parton distributions of the hadron (GPDs) <sup>43</sup>. The first form factor, corresponding to the first momentum of GPDs is the standard electromagnetic form factor -  $G(t)$ . The second form factor is determined by the second momentum of GPDs -  $A(t)$ . The parameters and  $t$ -dependence of the GPDs are determined by the standard parton distribution functions and hence experimental data on deep inelastic scattering and by experimental data for the electromagnetic form factors (see <sup>44</sup>).

The model takes into account two hadron form factors  $F_1(t)$  and  $A(t)$ , which correspond to the charge and matter distributions <sup>45</sup>. Both form factors are calculated as the first and second moments of the same Generalized Parton Distributions (GPDs). Hence, additional fitting parameters are not required for the description of the form factors.

The Born scattering amplitude has four free parameters (the constants  $C$ ) at high energy: two for the two pomeron amplitudes and two for the odderon. The real part of the hadronic elastic scattering amplitude is determined through the complexification  $\hat{s} = -is$  to satisfy the dispersion relations. The oscillatory function was determined <sup>15</sup>

$$f_{osc}(t) = h_{osc}(i + \rho_{osc}) J_1(\tau) / \tau; \quad \tau = \pi (\phi_0 - t) / t_0, \quad (6)$$

where  $J_1(\tau)$  is the Bessel function of the first order. This form has only a few additional fitting parameters and allows one to represent a wide range of possible oscillation functions.

After the fitting procedure we obtain  $\chi^2/n.d.f. = 1.24$  (remember that we used only statistical errors). One should note that the last points of the second set above  $-t = 2.8 \text{ GeV}^2$  show an essentially different slope, and we removed them. The total number of experimental points of both sets equals 415. If we remove the oscillatory function, then  $\chi^2/n.d.f. = 2.7$ , so an increase is more than two times. If we make a new fit without  $f_{osc}$ , then  $\chi^2/n.d.f. = 2.4$  decreases but remains large. However, this result was obtained with a sufficiently large additional coefficient of the normalization  $n = 1/k = 1.135$ . It can be for a large momentum transfer, but unusual for a small region of  $t$ .

Now let us put the additional normalization coefficient to unity and continue to take into account in our fitting procedure only statistical errors. Of course, we obtain an enormously huge  $\sum \chi^2$ . The new fit changes the basic parameters of the Pomeron and Odderon Born terms but does not lead to a reasonable size of  $\chi^2$ . We find that the main part of  $\sum \chi^2$  comes from the region of a very small momentum transfer. It requires the introduction of a new term which can help to describe the CNI region of  $t$ . This kind of term can be taken in different forms. In the present paper, we examined two different forms. One is the simple exponential form

$$F_d(t) = h_d(i + \rho_d)e^{-B_d|t|^\kappa \log \hat{s}}, \quad (7)$$

and the other is the power form which has  $t$ -dependence similar to the squared Coulomb amplitude.

$$F_d(t) = h_d(i + \rho_d)/(1 + (r_d t)^2) G_{el}^2. \quad (8)$$

where  $G_{el}^2$  is the squared electromagnetic form factor of the proton. For simplicity, in a further fitting procedure the constant  $\rho_{osc}$  and the phase  $\phi_0$  of the oscillatory term are taken equal to zero. Hence, the oscillatory term depends only on two parameters -  $h_{osc}$  and  $t_0$  period of oscillation. Also, to reduce the number of fitting parameters the correction to the main slope is taken in a simple form, we obtain the slope as

$$B(t) = \alpha' \log \hat{s}(1 - te^{B_{ad}t}). \quad (9)$$

The Pomeron trajectory has threshold singularities, the lowest one being due to the two-pion exchange required by the  $t$ -channel unitarity<sup>46</sup>. This threshold singularity appears in different forms in various models (see<sup>47,48</sup>) and is now recalculated by V. Khoze<sup>49</sup>. It can be shown that this term has a complicated structure and is determined by cancelation of two divergent terms with a small rest which we approximated by our small correction term to the main slope. This form leads to the standard form of the slope as  $t \rightarrow 0$  and  $t \rightarrow \infty$  and practically does not effect the rapidly decreasing additional term  $F_d(t)$ .

The fit of both sets of the TOTEM data simultaneously with taking into account only statistical errors, with additional normalization equal to unity and with the additional term, eq.(7), gives a very reasonable  $\chi^2 = 551/425 = 1.29$ . The results are present for the full region of  $t$  in Fig.1a, and with zoom of the region of small  $t$  in Fig.1b, and zoom of the region of the diffraction minimum in Fig.1c.

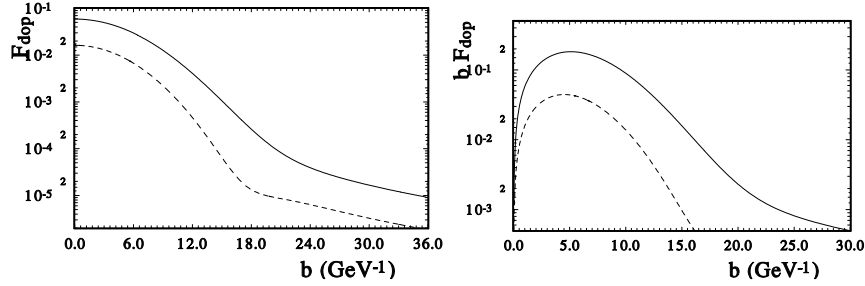


Fig. 2. The amplitude  $F_{dop}(b)$  eq.(7) in the impact parameter representation a) [left] the real  $F_{dop}(b)$ - hard line and imaginary part  $ImF_{dop}(b)$  -dashed line ; b) [right] overlapping function  $bF_{dop}(b)$  (hard line; imaginary part - dashed line).

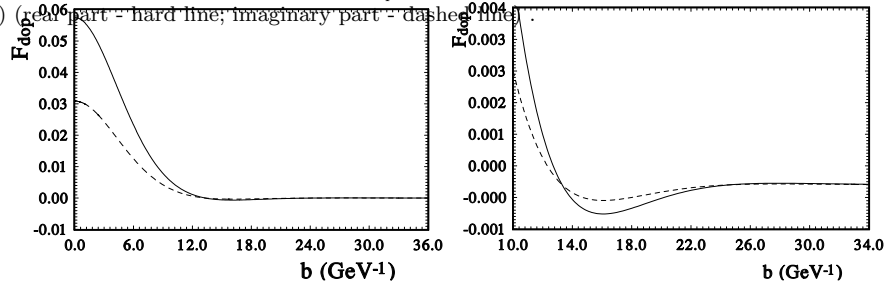


Fig. 3. The amplitude  $F_{dop}(b)$  eq.(8) in the impact parameter representation a) [left] the real  $F_{dop}(b)$ - hard line and imaginary part  $ImF_{dop}(b)$ -dashed line ; b) [right] the same at large impact parameters.

The parameters of the additional term are well defined  $h_d = 1.7 \pm 0.01$ ;  $\rho_d = -0.45 \pm 0.06$ ;

$$B_d = 0.616 \pm 0.026; \quad \kappa = 1.119 \pm 0.024.$$

Using the second form of the additional term, eq.(8), we obtain practically the same picture with the same  $\chi^2 = 549/425 = 1.28$  ( with the parameters of the additional term  $h_d = 1.067 \pm 0.044$ ;  $\rho_d = -0.53 \pm 0.07$

$$r_d = 7.62 \pm 0.34).$$

To check up the impact of the form of the CNI phase -  $\varphi(t)$ , we made our calculations with the original Bethe phase  $\varphi = -(dLOG(Bsl/2. * t) + 0.577)$  as well. We found that  $\sum \chi^2$  changes by less than 0.2% and practically does not impact the parameters  $F_d(t)$ . Hence, our model calculations show two possibilities in the quantitative description of the two sets of the TOTEM data. One - takes into account an additional normalization coefficient, which has a minimum size of about 13% ; the other - the introduction of a new anomalous term of the scattering amplitude, which has a very large slope and gives the main contributions to the Coulomb-nuclear interference

region.

Of course, there are some other ways to obtain good descriptions of the new experimental data of the TOTEM Collaboration. One is to use a model with an essentially increasing number of the fitting parameters and many different parts of the scattering amplitude. Another is to use a polynomial model with many free parameters. In both cases, the physical value of such a description is doubtful.

Let us examine the additional term in the impact parameter representation and use the Fourier transform

$$F_{dop}(b) \sim \int_0^\infty dq J_0(qb) F_{dop}(q^2), \quad (10)$$

The results for the additional term, in the form of eq.(7), are presented in Fig.2a. Figure 2b shows that the main contribution comes from the non-large impact parameters. The maximum of  $bF_{dop}(b)$  is situated in the region of  $r \sim 1\text{fm}$ , slightly above the electromagnetic radius of proton. Figure 3 shows the impact parameter representation for the real and imaginary parts of  $F_{dop}$ , in the form of eq.(8).

#### 4. Other models

The above results were obtained in the framework of one specific model. Let us see what other models tell us. There are many different models with very different paradigms (for example, see reviews<sup>48,19</sup>) and we take only some of them as an example. One of the oldest models, which is based on the hadron structure<sup>51</sup> is enclosed by the quark-antiquark cloud. The cloud becomes polarized because its antiquarks are drawn toward the baryonic shell. In turn, a layer of polarization quarks appears. In pp near forward scattering, the two outer layers collide leading to a new scattering amplitude (positive). In  $p\bar{p}$  near forward scattering, the outer polarization layer of the antiproton is of antiquarks and the polarization scattering amplitude is negative. Thus, polarization of the clouds incorporates a small crossing-odd amplitude into our diffraction amplitude. It says that the main result is " The most striking feature of the preliminary  $\sqrt{s} = 13$  TeV TOTEM data is that there are no oscillations in  $d\sigma/dt$  beyond the initial dip-bump structure. It shows a smooth falloff for large  $|t|$ , exactly as predicted by our model." The model gives, as many others, only a qualitative description of the differential cross section and does not feel the fine structure.

Some other models, for example<sup>52</sup>, developed the structure of the scattering amplitude, but in the analysis of the experimental data they do not include the specific properties of the hadron interaction at small momentum transfer - " Note that in this paper, we treat only the strong (nuclear) amplitude separated from Coulomb forces. The CNI effects modify the nuclear cross-section by less than 1% for  $|t| > 007$  GeV<sup>2</sup>; thus, in the nuclear range, the CNI effects can be ignored"

The same specific bounds were taken by one of the famous models<sup>53</sup>. In a recent paper they noted: " This paper applies it in its simplest form to small-  $t$  data from 13.76 GeV to 13 TeV for total cross sections and elastic scattering at small  $t$ , namely

$|t| < 0.1 \text{ GeV}^2$  by including in the amplitude the exchange of the soft pomeron  $|P$  of the reggeons  $\rho, \omega, f_2, a_2$  and of two pomerons  $IPIP$ . The fit reveals no need[3] for any odderon contribution at small  $t$ ." As in many other papers in <sup>53</sup> they speak only about a good fit, which is shown in different Figures. However, they do not speak about the sizes of  $\chi^2$ , especially in different regions of momentum transfer. It is interesting that in <sup>53</sup> they note " ...but the slope for 7 TeV data lies between that for 8 and 13 TeV, which is surely anomalous". Hence, all such models can not see some fine structure of hadron interactions, which is discussed in our paper, but note some anomalous behavior of the slope.

Some models include in the analysis the Coulomb-hadron interference region and note the importance of this region of  $t$ . However, in most part, they are interested in the deviation of the differential cross sections from the exponential form, which leads to some "break" in the region of  $-t \sim 0.15 \text{ GeV}^2$ . For example, in <sup>18</sup> they note - "The left plot shows the non-exponential behavior of the differential cross section for T8. ..." The figure is obtained subtracting from the best fit of the differential cross section with a pure exponential form  $Re(f) = Aexp(Bt)$  and dividing the subtraction by this reference function. The dashed lines show the normalization error band in  $d\sigma/dt$ , which is quite large. The plot in the RHS shows the ratio  $(T2 - R)/T2$  which exhibits information of a non-exponential behavior with advantages compared with the first plot, since is cancelled, and with it most of the normalization systematic error." It is interesting that they show the importance of systematic errors for a good description of the differential cross sections.

In a recent complicated work <sup>19</sup>, which based on the modified Barger-Philips scattering amplitude <sup>54</sup>, a qualitative description of the experimental data at  $\sqrt{s} = 7, 8, 13 \text{ TeV}$  in the near-forward region up to  $-t = 0.2 \text{ GeV}^2$  was obtained. One of the specific moment of the model is the use of the energy dependence of the hadron form factor. The obtained value of  $\sigma_{tot}(\sqrt{s} = 13 \text{ TeV}) = 113.66 \text{ mb}$  in the first variant and 111.09 in the fourth variant of the model; the corresponding values of  $\rho(t = 0)$  equal 0.133 and 0.134.

Another interesting model <sup>55</sup> examines modern experimental data of the TOTEM Collaboration. They used two-Pomeron eikonal approximation with soft and hard Pomeron. A specific feature of the model is that it uses the essentially nonlinear parametrization for the soft and hard pomerons of the Regge trajectory. With minimum fitting parameters obtained earlier ( via fitting to elastic scattering data in the collision energy range  $546 \text{ GeV} \leq \sqrt{s} \leq 7 \text{ TeV}$  ) the model gives a good qualitative description of the new experimental data at 13 TeV. After re-fitting parameters, it gives for the data at 13 TeV  $\sum \chi^2 = 980$ . The result is very interesting from our viewpoint. We present their Fig. 2b in our Fig.4. The difference between the model results and the experimental data at small momentum transfer is remarkable. Very likely that it shows the necessity of additional normalization of the experimental data or the existence of some anomaly in  $t$  dependence of the differential cross sections. =

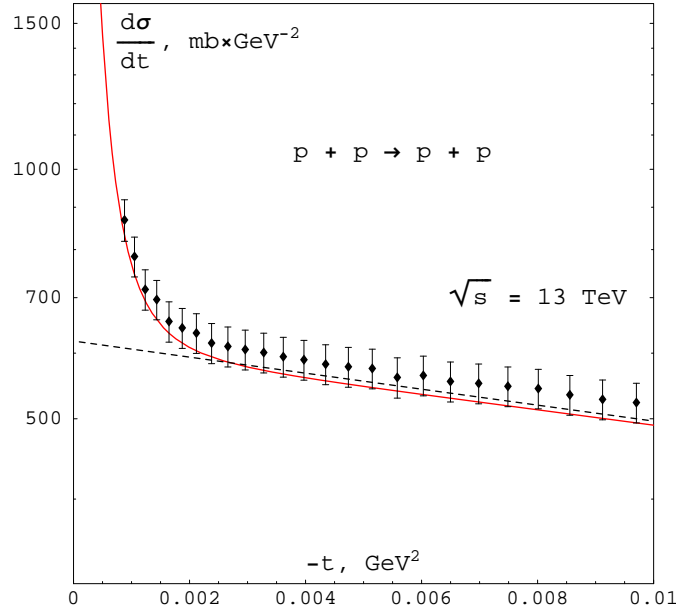


Fig. 4. from paper [39] "Figure 2: The predictions of the model [6] in the case  $HP(0) - 1 = 0.32$  versus the TOTEM data at  $\sqrt{s} = 13$  TeV [7]. The dashed line corresponds to the approximation  $C(s, t) = 0$ "

### 5. The fit of the differential cross section in the small momentum transfer region

Above, the examination of the new TOTEM experimental data at  $\sqrt{s} = 13$  TeV carried out in a wide momentum transfer shows the existence of some anomaly in the behavior of the differential cross sections at a very small momentum transfer. Of course, it has some dependence on the model structure. We cannot exclude a possibility of discovering a more complicated model that explains new features of hadron interactions at large distances. Hence, it is important also to see the phenomena of the new effect only in the small momentum transfer region and in the framework of the simplest form of the scattering amplitude. Now let us limit our examination to a small region of momentum transfer (up to  $-t = 0.069$ ) which includes 79 experimental data of the first set of the TOTEM Collaboration<sup>1</sup>. This region was examined by the TOTEM Collaboration and some other groups of researchers (for example<sup>5,10</sup>). Unlike other groups, we will take into account only statistical errors and the additional normalization  $k = 1$ . The new data of the TOTEM Collaboration have very small statistical errors, especially in the low momentum region. Hence, our fitting procedure will give the non-small  $\sum \chi_i^2$ ; however, it imposes hard restrictions on different representations of the scattering amplitude. Firstly, let us

examine the Born scattering amplitude using the standard eikonal representation, as was made in our model analysis of the whole region of the momentum transfer of experimental data.

Let us take the hadronic Born scattering amplitude in the simple exponential form. Of course, after eikonalization such an amplitude is added the standard electromagnetic amplitude, as we made in the model analysis,

$$F_{\mathbb{P}}(s, t) = h/(2 \cdot 0.389\pi)(i + \rho)Exp(B/2t) \quad (11)$$

As was made in a recent work<sup>10</sup>, we will made the fit in different regions of  $t$ . Our results are given in Table 1. Table 1 and the following tables show the sizes of  $\sum \chi^2$  and the integrated probability -  $p$  - *value* (the area under  $\chi^2$  probability density function (pdf) to the right of the minimum  $\chi^2$  value (see, for example,<sup>56</sup>). The maximum width of the examined region leads to the non-small  $\sum \chi_i^2$ . It is shown that a simple exponential form is not sufficient for our analysis. Of course, when we come to a small region of  $t$ , the description is improving more and more. It is to be noted that the size of the slope has small variation with decreasing  $t$ . In our analysis, the slope size is somewhat less than was determined by the TOTEM group<sup>1</sup> and by the Protvino group<sup>10</sup>. This may be the result of the slope determined by the Born scattering amplitude that is further changed by the eikonalization procedure. However, we are interested in the possibility of the contribution of an additional rapidly decreasing term of the scattering amplitude.

Let us add an additional term in the form

$$F_{ad}(s, t) = i h_d/(2 \cdot 0.389\pi) e^{D_{at}} \quad (12)$$

This form correspond to eq.(7) but with some simplification as the narrow region of momentum transfer requires minimum fitting parameters. As a result, two additional parameters appear in the fitting procedure. We reduce the real part of the additional term as the increase in the number of the fitting parameters leads to large uncertainty in the results. It should be noted that if we add two additional parameters in the main Born amplitude as additional slopes -  $B_1 \sqrt{-t}$  and  $B_2 t^2$ , this will not practically change the picture. The same result was obtained by the TOTEM Collaboration, too.

The results of our new fitting are presented in Table 2. The  $\chi^2$  decreases is essential, especial for the completely examined  $t$  region. The constant of the additional term is determined sufficiently well. The slope of the additional term is large and also is determined with small errors.

The  $\chi^2(t)$  are shown in Fig.5 in the case of taking into account the additional fast decreasing term (dashed line) and in the case of the absence of such a term (hard line). We can see that the largest difference comes from a very small region of momentum transfer.

Let us include additional normalization (representing systematical errors) in our fitting procedure. The dependence of  $\sum_i^N \chi^2$  on the additional coefficient of normal-

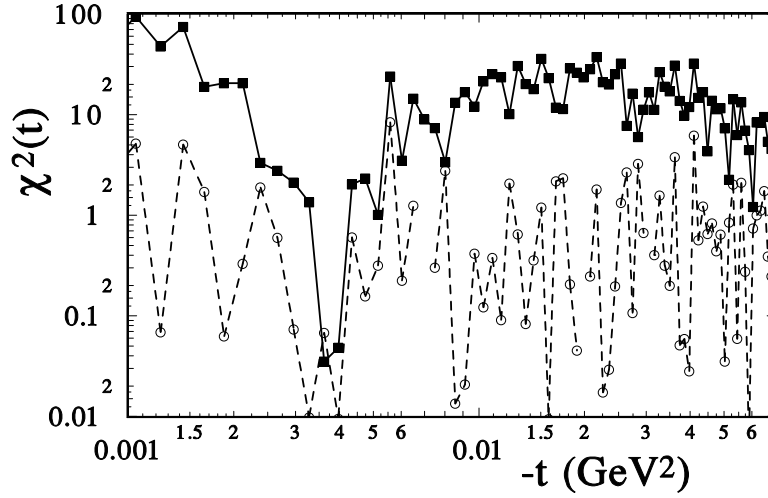


Fig. 5. The  $\chi^2(t)$  in the case of taking into account the additional fast decreasing term (dashed line) and in the case of the absence of such a term (hard line).

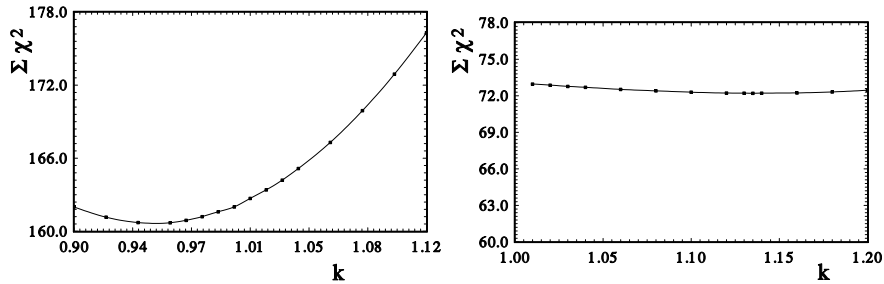


Fig. 6. The dependence of  $\chi^2$  on the additional normalization coefficient of experimental data - a) [top] in the case of the simple exponential form of the scattering amplitude; b) [bottom] the same but with the additional fast decreasing term.

ization of experimental data is shown in Fig. 6. The case of the simple exponential for the scattering amplitude is presented at the top of Figure 4; and with the additional fast decreasing term at the bottom. One can see that  $\chi^2$  in the first case essentially depends on the normalization coefficient and has a sufficiently large value (remember that we used only statistical errors). Note that  $k = 1/n$  is the coefficient by which we multiply our theoretical function to compare with experimental data in our fitting procedure. The minimum is reached when the additional normalization equals 13.5%. This corresponds to the additional normalization which was used in

Table 1. The fit of  $d\sigma/dt$  by the Born hard scattering amplitude in one exponential form using the eikonal representation.

N	$-t_{max}(GeV^2)$	$\sum \chi_i^2$	$\chi_{dof}$	pdf	h (GeV <sup>-1</sup> )	B(GeV <sup>-2</sup> )
79	0.0699	162.1	2.19	2.5E-8	110.2 ± 0.3	16.0 ± 0.03
70	0.0559	86.5	1.29	0.055	110.5 ± 0.4	16.4 ± 0.04
65	0.0488	66.3	1.07	0.331	110.6 ± 0.6	16.3 ± 0.05
60	0.0422	55.3	0.97	0.539	110.6 ± 1.4	16.4 ± 0.06
55	0.0361	49.7	0.96	0.565	110.6 ± 1.7	16.4 ± 0.08
50	0.0305	47.8	1.02	0.440	110.6 ± 1.4	16.4 ± 0.1
40	0.0207	34.2	0.92	0.601	110.7 ± 0.6	16.6 ± 0.2

 Table 2. The fit of  $d\sigma/dt$  by the Born hard scattering amplitude in two exponential form using the eikonal representation.

N	$-t_{max}(GeV^2)$	$\sum \chi_i^2$	$\chi_{dof}$	pdf	h (GeV <sup>-1</sup> )	$D_d(GeV^{-2})$
79	0.0699	74	1.00	0.478	3.26 ± 0.3	41.2 ± 1.9
70	0.0559	62.2	0.93	0.575	2.94 ± 0.4	39.2 ± 4.1
65	0.0488	56.8	0.94	0.593	2.26 ± 0.6	31.6 ± 5.8
60	0.0422	53.0	0.96	0.550	1.51 ± 1.4	25.3 ± 7.7
55	0.0361	49.0	0.98	0.513	1.56 ± 1.7	25.5 ± 11.4
50	0.0305	44.4	0.98	0.497	1.93 ± 1.4	29.7 ± 13.7
40	0.0207	33.0	0.94	0.565	2.4 ± 0.6	29.7 <sub>fixed</sub>

 Table 3. The comparison of  $\sum \chi_i^2$  from the fit of  $d\sigma/dt$  by the hard scattering amplitude in the exponential and two exponential forms.

N	$-t_{max}(GeV^2)$	$\sum \chi_i^2$ (Exp)	pdf	$\sum \chi_i^2$ (Exp+fd)	pdf	$h_d$
79	0.0699	67.61	0.686	62.87	0.818	1.95 ± 0.35
70	0.0559	61.52	0.600	59.24	0.678	2.14 ± 0.58
65	0.0488	57.14	0.628	55.32	0.647	2.25 ± 0.73
60	0.0422	54.51	0.490	52.90	0.550	2.36 ± 0.95
55	0.0361	50.26	0.460	48.39	0.498	2.03 ± 0.82
50	0.0305	45.22	0.463	41.67	0.613	1.35 ± 0.54
45	0.0254	38.03	0.569	34.58	0.712	2.33 ± 1.35
40	0.0207	35.02	0.467	32.45	0.592	1.95 ± 1.35

our HEGS model calculations without the additional fast decreasing term. Contrary, in the case with the additional term the dependence on normalization is weak and the size of  $\chi^2$  has a reasonable value in a wide region of normalization.

Now let us carry out analysis without eikonalization. In this case, the additional term will be represented in the power form (like a square of Coulomb amplitude)

$$F_{ad}(s, t) = \alpha_{el}^2 h_d / (2 \cdot 0.389\pi) / [\epsilon + t^2] \quad (13)$$

where  $\alpha_{el} = 1/137$  is the electromagnetic fine structure constant and  $\epsilon$  is free parameter order  $\alpha_{el}^2$ . This form corresponds to eq.(8) but in the form more close to the screening Coulomb amplitude, as it is remarkably close to the form of the

Coulomb amplitude but without the divergence at  $t \rightarrow \infty$ . The comparison of  $\chi^2$  for a simple exponential term and with the added fast decreasing term are presented in Table 3. The difference is not large; however, it is about 10% for every examined region of  $t$ . The constant  $h_d$  is also well determined.

## 6. Conclusion

Using only statistical errors and fixing additional normalization of differential cross sections equal to unity, we have limited the possible forms of the theoretical representation of the scattering amplitude. The phenomenological model - HEGSh model was used for examining the whole region of the momentum transfer of two sets of experimental data obtained by the TOTEM Collaboration at 13 TeV. The simple exponential form of the scattering amplitude was used to examine only a small region of momentum transfer. In both cases, an additional fast decreasing term of the scattering amplitude was required for a quantitative description of the new experimental data. The large slope of this term can be connected with a large radius of the hadronic interaction and, hence, can be determined by the interaction potential at large distances. It can be some part of the hadronic potential responsible for the oscillation behavior of the elastic scattering amplitude<sup>15</sup>.

The discovery of such anomaly in the behavior of the differential cross section at very small momentum transfer in LHC experiments will give us important information about the behavior of the hadron interaction potential at large distances. It may be tightly connected with the problem of confinement. We have shown the existence of such anomaly at the statistical level and that some other models also revealed such unusual behavior of the scattering amplitude. Very likely, such effects exist also in experimental data at essentially smaller energies<sup>50</sup>. However, the results of the TOTEM Collaboration have a unique unprecedentedly small statistical error and reach minimally small angles of scattering with the largest number of experimental points in this small region of the momentum transfer. The new effects can impact the determination of the sizes of the total cross sections, the ratio of the elastic to the total cross sections and the size of the  $\rho(s, t)$  - the ratio of the real to imaginary part of the elastic scattering amplitude.

Now the results for the total cross sections and  $\rho(t = 0)$  can be compared for the case with additional coefficient normalization  $k$  and the cases with an additional fast decreasing term and  $k = 1$ . The results are presented in Table IV. The different variants with a large coefficient of the normalization give practically the same value, which is less than the total cross sections extracted by the TOTEM Collaboration -  $\sigma_{tot(TOTEM)} = 110.6 \pm 3.4$  mb in the analysis of only small momentum transfer region<sup>57</sup>. Small errors of  $\rho(t = 0)$  and  $\sigma_{tot}$  are the result of our simultaneous fitting to both sets in a wide region of the momentum transfer and with using only statistical errors. The size of  $\rho(t = 0)$  obtained in the model calculations essentially exceed the size of  $\rho(t = 0) = 0.1 \pm 0.01$  extracted by the TOTEM Collaboration<sup>58</sup>. On the contrary, the variants with an additional fast decreasing term in different

Table 4. A comparison of  $\sigma_{tot}(\sqrt{s} = 13 \text{ TeV})$  and  $\rho(t = 0, \sqrt{s} = 13 \text{ TeV})$  obtained in the different variants of the model calculations.

n	model	$\sum \chi_i^2/N$	$10^4 \times \text{pdf}$	$\sigma_{tot} \pm \text{err}$ (mb)	$\rho(t = 0) \pm \text{err}$
1.135		525/415	0.8	$106.1 \pm 0.2$	$0.146 \pm 0.004$
1.135	$f_d = 0$	515/425	6.5	$106.2 \pm 0.2$	$0.142 \pm 0.004$
1.135		527/425	2.3	$106.2 \pm 0.2$	$0.148 \pm 0.004$
1.	$f_d(r_d)$	539/425	0.3	$113.2 \pm 0.106$	$0.109 \pm 0.004$
1.	$f_d(r_d)$	549/425	0.1	$113.1 \pm 0.106$	$0.113 \pm 0.004$
1.	$f_d(Exp)$	550/425	0.1	$112.6 \pm 0.107$	$0.115 \pm 0.004$

forms give a large value of  $\sigma_{tot}(\sqrt{s} = 13 \text{ TeV})$  which exceeds the  $\sigma_{tot}(TOTEM)$ , and  $\rho(t = 0)$  practically coincides with the predictions of the COMPETE Collaboration<sup>59</sup>. Now many different groups using the TOTEM Collaboration data obtained different results for  $\rho(t = 0)$  and  $\sigma_{tot}$ . When they used only small -t data, the results were not far from the TOTEM data for  $\sigma_{tot}$  but essentially differed for  $\rho(t = 0)$  (see, for example,<sup>10</sup>).

In<sup>60</sup> the TOTEM Collaboration notes that the two combined TOTEM results yield  $\sigma_{tot} = 110.5 \pm 2.4 \text{ mb}$ . It means that our model calculations (see Table 4) differ by two  $\sigma_{errTOTEM}$  for the case with large additional normalization and by one  $\sigma_{errTOTEM}$  for the case where the additional normalization is fixed by unity. Note that in the model calculations only statistical errors were used.

Of course, we can not exclude the case that the real experimental normalization reaches essentially larger values than taken into account by the TOTEM Collaboration. However, for a small momentum transfer it is a very unlikely case, as practically in all existing experiments on measurement of the differential cross sections at the small momentum transfer systematic errors do not exceed a few percent.

**Acknowledgements** *The authors would like to thank Jean-Rene Cudell for fruitful discussion of some questions considered in the paper.*

## References

1. G. Antchev *et al.* [TOTEM Collaboration], arXiv:1812.04732 [hep-ex].
2. G. Antchev *et al.* [TOTEM Collaboration], arXiv:1812.08283 [hep-ex].
3. E. Martynov, B. Nicolescu, Phys.Lett. bf B778 414 (2018).
4. V. A. Khoze, A. D. Martin, M. G. Ryskin, Phys. Rev. D 97, 034019 (2018)
5. J.-R. Cudell, O.V. Selyugin, arXiv: 1901.05863 [hep-ph].
6. G. Auberson, T. Kinoshita, A. Martin, *Phys. Rev.* **D3**, 3185 (1971).
7. J. Fischer, *Phys.Rep.* **76**, 157 (1981).
8. S.M. Roy, *Phys.Lett.* **B 34**, 407 (1971).
9. I.M. Dremin, Physics1(1), 33 (2019).
10. V.V. Ezhela, V.A. Petrov, N.P. Tkachenko, arxiv: 2003.03817 [hep-ph].
11. O. Selyugin, Phys. Lett. **B333**,(1994) 245.
12. J. R. Cudell and O. V. Selyugin, Phys. Rev. Lett. **102** (2009) 032003 [arXiv:0812.1892 [hep-ph]].
13. O. V. Selyugin, Eur. Phys. J. C **72**, 2073 (2012).

14. O. V. Selyugin, Phys. Rev. D **91**, no. 11, 113003 (2015)
15. O.V. Selyugin, Phys.Lett.**B797** 134870 (2019).
16. E. Ferreira, A. K. Kohara, J. Sesma, Phys. Rev. C **97**, 014003 (2018)
17. E. Gotsman, E. Levin, I. Potashnikova, Phys. Rev. D **101** 094021 (2020).
18. A. K. Kohara, E. Ferreira, T. Kodama and M. Rangel, Eur.Phys.J. C **77** 877 (2017).
19. G.Pancheri, S. Paccetti, V. Strivasta, Phys.Rev. **D99** 2019, 034014.
20. C. Bourrely, J. Soffer, T.T. Wu, Nucl. Phys. B **247**, 15 (1984)
21. C. Bourrely, Eur.Phys.J. C **74**, 2736 (2014).
22. R. Orava, O. V. Selyugin, arXiv:1804.05201 [hep-ex]
23. D. Stump, J. Pumplin, R. Brock, D. Casey, J. Huston, J. Kalk, H.L. Lai and W.K. Tung, Phys. Rev. D **65** 014012 (2001).
24. P. Jimenez-Delgado, Phys.Lett. **B714** 301 (2012).
25. K. J. Eskola et al., Eur.Phys.J., **C77** (2017) 163; [arXiv:1612.05741].
26. F. Kohlinger, H. Hoekstra, and M. Eriksen, Mon Not R Astron Soc (2015) 453 (3): 3107-3119; [arXiv:1508.05308].
27. I.M. Sitnik, Comp.Phys.Comm., **209** 199 (2016).
28. I.M. Sitnik, I.I. Alexeev, O.V. Selyugin, Comp.Phys.Comm., **251** 107202 (2020).
29. I.N. Silin, CERN Program Library, D510, FUMILI, (1983).
30. J. R. Cudell, O. V. Selyugin, arXiv:1901.05863 hep-ph.
31. O.V. Selyugin, Mod. Phys. Lett. A **9** (1994) 1207.;
32. O.V. Selyugin, Mod. Phys. Lett. A **11** (1996) 2317;
33. O.V. Selyugin, Phys. Rev. D **60** (1999) 074028.
34. O. V. Selyugin, Nucl.Phys. A **959** (2017) 116.
35. J.-R. Cudell, O.V. Selyugin, Aip Conf.Proc. **1350**: 115 (2011); arxiv: 0811.4369; arXiv:1011.4177.
36. O. V. Selyugin, J.-R. Cudell, arxiv: 1810.11538; Proceedings of the conference Diffraction and Low-x 2018, Reggio Calabria, Italy, August 26th t- September 1st, 2018; O.V. Selyugin, Acta Phys Pol. B (proc.Supl.) v.12, p.741 (2019)
37. C. Bourrely, J. Soffer, T.T. Wu, Eur.Phys.J. **C28** (2003) 97.
38. H. Miettinen, Nucl.Phys. B **166** (1980) 365.
39. H. Pagels, Phys.Rev. **144** (1966) 1250).
40. W. Broniowski, E.-R. Arriola, Phys.Rev. **D78**, 094011 (2008).
41. X.D. Ji, Phys. Lett. **78** , (1997) 610; Phys. Rev D **55** (1997) 7114.
42. Radyushkin, A.V., Phys. Rev. D **56**, (1997) 5524.
43. O.V. Selyugin, Proceedings Intern. Conf. "SPIN in High Energy Physics", Dubna (2012), Particles & Nuclei, **45** 39 (2014).
44. O.V. Selyugin and O.V. Teryaev, Phys.Rev. **D 79** 033003 (2009).
45. O.V. Selyugin, Phys. Rev., **D 89** (2014) 093007.
46. A. Anselm and V. Gribov, Phys. Lett. **B40**, 487 (1972).
47. G. Cohen-Tannoudju *et al.* Lett. Nuovo Cim. **5** (1972) 957;
48. R. Fiore, L. Jenkovszky, R. Orava, E. Predazzi, A. Prokudin, O. Selyugin, Mod.Phys., A24: 2551-2559 (2009)
49. V.A. Khoze, A.D. Martin and M.G. Ryskin, arxiv:hep-ph/0007359.
50. O. V. Selyugin, J.-R. Cudell, Mod.Phys.Lett. A27, (2012)1250113; arxiv: 1207.0600.
51. M. Islam, , arXiv -1709.03172
52. I. Szanyi, L. Jenkovszky, R. Schicker, V. Svintozelskyi, Nuclear Physics A **998** (2020) 121728.
53. A. Donnachie, P.V. Landshoff, DAMTP-19-18, arXiv:1904.11218.
54. R.J.N. Philips and V.D. Barger, Phys.Lett. **B46** 412 (1973).
55. A. Godizov, Phys.Rev. **D101**074028 ( 2020). Phys. Rev. D **101**, 074028 (2020)

56. D.J. Hudson, "STATISYICS - Lectures on Elementary Statistics and Probability", Geneva (1964).
57. TOTEM Collab., G. Antchevet al., " $\sqrt{s} = 13$ " TeV by TOTEM and overview of cross-sectiondata at LHC energies," arXiv:1712.06153 [hep-ex].
58. TOTEM Collab., G. Antchevet al., CERN-EP-2017-335.
59. J.-R. Cudel et all (COMPETE Collaboration) Phys.Rev. J. R. Cudell *et al.* [COMPETE Collaboration], *Phys. Rev.D*, **65**, 074024 (2002).
60. TOTEM Collab., G. Antchevet al., arxiv: 1812.04732.

